J Mol Model (2011) 17:1911–1918
DOI 10.1007/s00894-010-0899-x

ORIGINAL PAPER

Probing solvation decay length in order to characterize hydrophobicity-induced bead–bead attractive interactions in polymer chains

Siddhartha Das · Suman Chakraborty

Received: 22 September 2010 / Accepted: 9 November 2010 / Published online: 26 November 2010

Abstract In this paper, we quantitatively demonstrate that exponentially decaying attractive potentials can effectively mimic strong hydrophobic interactions between monomer units of a polymer chain dissolved in aqueous solvent. Classical approaches to modeling hydrophobic solvation interactions are based on invariant attractive length scales. However, we demonstrate here that the solvation interaction decay length may need to be posed as a function of the relative separation distances and the sizes of the interacting species (or beads or monomers) to replicate the necessary physical interactions. As an illustrative example, we derive a universal scaling relationship for a given solute–solvent combination between the solvation decay length, the bead radius, and the distance between the interacting beads. With our formalism, the hydrophobic component of the net attractive interaction between monomer units can be synergistically accounted for within the unified framework of a simple exponentially decaying potential law, where the characteristic decay length incorporates the distinctive and critical physical features of the underlying interaction. The present formalism, even in a mesoscopic computational framework, is capable of incorporating the essential physics of the appropriate solute-size dependence and solvent-interaction dependence in the hydrophobic force estimation, without explicitly resolving the underlying molecular level details.

Keywords Hydrophobicity · Solvation · Collapse

S. Das · S. Chakraborty (✉)
Department of Mechanical Engineering,
Indian Institute of Technology,
Kharagpur 721302, India
e-mail: suman@mech.iitkgp.ernet.in

Introduction

The effective attraction between large apolar groups in water plays a critical role in the stability of complex biological structures in aqueous environments. For example, interactions between large assemblies or relatively high concentrations of hydrophobic groups in water dictate the transition of a polymer from a diffuse coiled state to a more compact ("collapsed") state. This is a classic example of monomer–monomer hydrophobic attractive interactions minimizing the interfacial and bending energies, thereby forcing the polymer molecule to undergo a phase transition. A plethora of investigations into the mechanisms of hydrophobic attraction-induced collapses of nanoscopic and microscopic moieties and the resulting changes in the free energies can be found in the literature [1–6]. The physics involved becomes even more complicated when there are charges on (or in the vicinity of) the interacting substances [7–14]. The presence of these charges induces a competition between hydrophobic and coulombic interactions that eventually dictate the final configuration of the system. In this study, however, the hydrophobic units are assumed to be uncharged, and all the derivations are obtained accordingly.

Hydrophobic interactions between monomer units in a polymer are likely to be rather complex. Consequently, it is rather difficult to represent this phenomenon by an integrated physical picture involving a simple interaction potential and a unique interaction length scale (there have been many studies that have considered the appropriate invariant length scales for hydrophobic interactions [15–18]). However, in a number of cases, it may be convenient to represent hydrophobic interactions between structural units through simple yet physically consistent and mathematically closed forms of equivalent interaction forces.

Such representations of interaction potentials may turn out to be essential elements in particle-based or mesoscopic simulations, as they enhance the computational tractability of the mathematical formulation without sacrificing the essential physics. Examples of these kinds are plentiful in the literature on Brownian dynamics simulations (BDS) of polymeric systems (such as spring force interaction potentials, harmonic bending potentials, etc.). In fact, in several of our recent studies [19, 20], we attempted to derive system parameters [by comparing the results of BDS with those obtained from molecular dynamics simulation (MDS) of an equivalent system] that effectively allow polymer interactions to be captured at extremely small length scales (which could have otherwise required explicit modeling of the solvent interactions) through the BDS formalism. What is still missing, though, is an accurate yet simple closed-form mathematical representation of hydrophobic interaction potentials for such cases that can quantitatively reproduce the detailed consequences of the underlying interaction mechanisms (such as effects of solute size or solvent interactions). Such a representation would not require the interaction parameters to be estimated through comparison with an equivalent MDS study [19, 20]; rather, it would be able to predict the parameters that govern the hydrophobic interactions by considering the physical conditions that trigger the hydrophobic collapse. With the above motivation, we have attempted to represent bead–bead hydrophobic interactions through closed mathematical forms. Different choices for the shape of the potential function may be plausible to achieve this aim in principle, provided that they can accurately represent the essential physics from both qualitative and quantitative perspectives. For instance, one can attempt to represent hydrophobicity-mediated *attractive interactions* between monomeric units in a polar solvent through an exponential form of the interaction potential [20, 21]:

$$U^{Solv} = \widetilde{u}_0 \exp\left(-\frac{\left|\Delta \mathbf{R}_{ij}\right|}{R_{attr}}\right) \tag{1}$$

where U^{Solv} is the attractive potential per unit area (J/m^2), $\widetilde{u}_0$ is expressed in units of $k_B T/\sigma^2$ (k_B is the Boltzmann constant, T is the absolute temperature and σ is the Lennard–Jones (LJ) length scale), $\Delta \boldsymbol{R}_{ij}=\boldsymbol{R}_i-\boldsymbol{R}_j$ is the position vector joining the centers of the beads i and j in the framework of a bead-spring model, and R_{attr} is the solvation decay length, which characterizes the range of the solvation interaction. It has been argued in the literature that choosing different characteristic decay lengths is not likely to alter the stable and metastable states of wormlike chains in a poor solvent [21–28]. However, when considering the implications of this, the thermophysical details of hydrophobic interactions between monomer units have been somewhat overlooked.

In the present paper, we consider the details of solvation interactions between hydrophobic monomer units in a poor solvent. We demonstrate that the generic form of the attractive potential, as given by Eq. 1, can appropriately capture the bead–bead hydrophobic interactions (for different physical conditions) provided that the parametric dependencies in R_{attr} are represented in a self-consistent fashion. In a system where hydrophobic effects dominate, we demonstrate that, despite an apparent universality in the exponentially decaying form chosen to mimic the resulting attractive interactions, the solvation decay length scale is solely responsible for representing the background physics in a quantitatively accurate manner. Consistent with this conjecture, we demonstrate a postulation of the parameter R_{attr} as a general function of the pertinent physical parameters, ensuring that the size dependence and the solvent-interaction dependence of the hydrophobic attraction are suitably represented even in a framework that includes the solvent interactions in a coarse-grain manner. This postulation contrasts sharply with the standard models commonly considered in the literature, in which the parameter R_{attr} (or its equivalent form; when the attractive potential is described by the LJ interaction, this becomes the molecular length scale) is routinely taken as a constant, and is thus insensitive to the details of the interaction mechanisms from which it derives [21–37]. The repulsive potentials (such as excluded volume interactions) may be treated separately and trivially. It is also important to mention in this context that the objective of this study is not to solve a polymer dynamics problem by considering all pertinent interaction forces. Rather, we aim to develop a simple guideline for effectively modeling inter-bead hydrophobic interaction potentials that may be employed in conjunction with other pertinent interaction forces in order to solve a problem of that kind. The usefulness of the proposed calculation is established by demonstrating how it can reproduce the MDS results of size-dependent or solvent-interaction-dependent hydrophobic effects in a mesoscopic framework. Consequently, the present formalism can be considered an important step towards the computationally efficient molecular modeling of hydrophobic systems involving extremely small length scales, which would otherwise invariably require the explicit modeling of solvent–solvent interactions.

Mathematical modeling

We begin our analysis by appealing to the standard idea that severe perturbations to hydrogen-bond networks around densely populated hydrophobic units may lead to the

formation of liquid-depleted layers in-between them. The interfacial fluctuations that separate the dense and depleted phases are likely to destabilize and expel the surrounding liquid, leading to an attraction between the hydrophobic units due to the resulting pressure imbalance. Such pressure imbalances, as driven by small-scale density fluctuations, may be assumed to follow Gaussian statistics with a variance of $\chi\left(\vec{r}, \vec{r}^{/}\right) = < \delta\rho\left(\vec{r}\right)\delta\rho\left(\vec{r}^{/}\right) >$, where $\delta\rho$ is the difference between the fluctuating molecular density field (n) and its slowly varying ensemble-averaged counterpart (n_s). For the sake of completeness, we first reproduce the important derivations governing the distributions of n, n_s, and the hydrophobic interaction potential, as discussed in Lum et al. [38]. The solvation free energy of the system, which is dictated by the probability of finding empty volumes in unperturbed fluids due to the presence of hydrophobic units, may be expressed as a ratio of the pertinent partition functions, leading to the following expression for an excess equivalent chemical potential:

$$U^{Hyd} = \Delta\mu_{ex} = -k_B T \ln\left[\frac{Z_v(0)}{\sum\limits_{N\geq 0} Z_v(N)}\right] \tag{2}$$

where $Z_v(N)$ is the partition function for the case when N solvent molecules occupy a volume v (volume occupied by the hydrophobic unit). This is given by [38]:

$$Z_v(N) = \exp\left\{-F\left(n_s\left(\vec{r};N\right)\right)/k_B T - \left(N - \int\limits_v d\vec{r}\, n_s\left(\vec{r};N\right)\right)^2 /2\sigma_v - \left(\ln\sigma_v\right)/2\right\} \tag{3}$$

In Eq. 3, F is the free energy functional, given by

$$F = \int d\vec{r}\left[w(n_s) + \frac{m}{2}|\nabla n_s|^2\right]. \tag{4}$$

In Eq. 4, w is the local free energy density referenced by the ambient chemical potential μ, and $m = a\lambda^2$ [39]. For free energy calculations, one can use a convenient van der Waals form [39]:

$$w(n) = nk_B T \ln\left(\frac{bn}{1-bn}\right) - an^2 - \mu n \tag{5}$$

with an interfacial energy constraint given by

$$\gamma_{lg} = \int\limits_{n_g}^{n_l} dn\sqrt{2m\left[w(n) - w\left(n_g\right)\right]} \tag{6}$$

where n_g and n_l are the bulk gas and liquid densities, respectively, at the liquid–gas coexistence state dictated by Eq. 5. Considering that the value of n_l is given by the density of liquid water at phase coexistence when T= 298 K, $\gamma_{lg} = 72\,\mathrm{MJ/m^2}$, and the compressibility implied by Eq. 5 has the same value as that for water under normal conditions [38], it follows that a=230 kJ cm^3 mol^{-2} and b= 15 cm^3 mol^{-1}, $\lambda = \sqrt{\frac{b}{a}} = 0.38\,\mathrm{nm}$. Further, the variance $\chi\left(\vec{r}, \vec{r}^{/}\right)$ may be expressed as

$$\chi\left(\vec{r}, \vec{r}^{/}\right) = n_s\left(\vec{r}\right)\delta\left(\vec{r} - \vec{r}^{/}\right) + n_s\left(\vec{r}\right)n_s\left(\vec{r}^{/}\right)h\left(\left|\vec{r} - \vec{r}^{/}\right|\right) \tag{7}$$

where $h\left(\left|\vec{r} - \vec{r}^{/}\right|\right) + 1$ is the radial distribution function of liquid water at the bulk density n_l [40]. The variable n_s can be computed using the following governing equation [38]:

$$\frac{\partial w}{\partial n_s\left(\vec{r}\right)} = m\nabla^2 n_s\left(\vec{r}\right) + 2a\left[\overline{n}\left(\vec{r}\right) - \overline{n}_s\left(\vec{r}\right)\right] \tag{8}$$

where bars over quantities denote coarse-grained density values, and

$$n\left(\vec{r};N\right) = n_s\left(\vec{r};N\right) - \int\limits_v d\vec{r}^{/} \int\limits_v d\vec{r}^{//}\left[n_s\left(\vec{r};N\right) - \frac{N}{v}\right]\sigma_v^{-1}\chi\left(\vec{r}^{//}, \vec{r}\right) \tag{9}$$

Using Eqs. 2–9, a plot of U^{Hyd} as a function of the separation distance (x) between two planar hydrophobic units may be obtained, as depicted in Fig. 1. From the figure, it is evident that water will remain between the two hydrophobic units until x becomes so small that the liquid becomes thermodynamically unstable.

The next objective of the analysis would be to translate the above picture of hydrophobic interactions

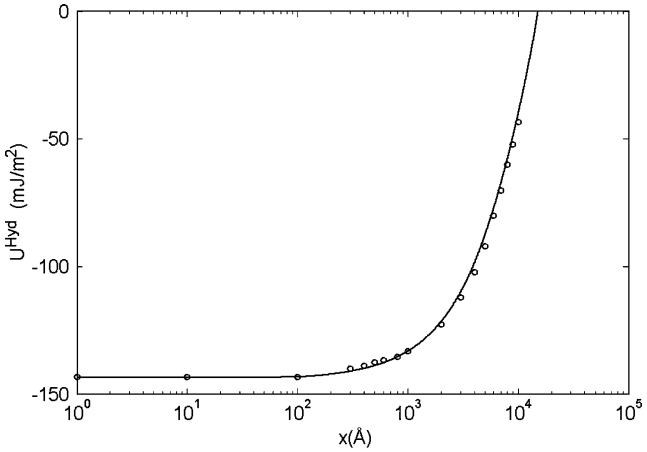

Fig. 1 Mathematical fit (given by Eq. 13; shown by *continuous line*) of the hydrophobic interaction potential obtained from [38] (marked by *circles*) between two plane surfaces as a function of the separation distance (x)

between planar surfaces into the equivalent for spherical units. Although a significant number of investigations concerning the hydrophobic solvation attractions between spherical units at different length scales have been reported in the literature [41–44], closed-form expressions for the pertinent interaction potential as a function of the separation distance—encompassing different ranges of the spheres' radii—have been missing. This lack of explicit relationships has often tempted researchers into employing heuristic forms of the interaction potential concerned without explicitly specifying the pertinent model parameters. Here, we attempt to overcome such shortcomings by extending the detailed thermophysical analysis of hydrophobic interactions between planar surfaces presented earlier to spherical geometries (thus essentially representing the beads in a polymeric unit). Note that the net hydrophobic interaction between two spherical units (with identical radii) as a function of their center-to-center distance r is then [45]

$$U^{Hyd,Sphere}(r) = U_1^{Hyd} - 2U_2^{Hyd} + U_3^{Hyd} \tag{10}$$

where U_1^{Hyd} results from the interaction between the front halves of the spheres (the halves that face each other), U_3^{Hyd} results from the interaction between the rear halves of the spheres (the halves that do not face each other), whereas U_2^{Hyd} results from the interaction between the front half of one sphere and the rear half of the other sphere. Since the interaction between two bodies strictly depends on their net exposed hydrophobic surface area [46–48], we can neglect the interaction energies U_2^{Hyd} and U_3^{Hyd}, so that

$$U^{Hyd,Sphere}(r) \approx U_1^{Hyd} \tag{11}$$

where

$$U_1^{Hyd} = 2\pi \int_0^{a_{rad}} \left(\sqrt{1-\frac{r^{/2}}{a_{rad}^2}}\right) U^{Hyd}\left(r - 2a_{rad}\sqrt{1-\frac{r^{/2}}{a_{rad}^2}}\right) r^{/}\, dr^{/} \tag{12}$$

Here a_{rad} is the radius of the spherical bead, and for analytical convenience $U^{Hyd}(x)$ may be described by a suitable curve fit (this is merely a mathematical fit that depicts the general characteristic trends obtained by solving the coupled Eqs. 2–9 for flat geometries, considering the physical properties of water) of Fig. 1:

$$\begin{aligned} U^{Hyd}(x) &= B\tanh[k(x-C)] && \text{for } x \le 100\text{Å} \\ &= B\tanh[k(x-C)] + A\sin\left[\pi\left(\tfrac{x-100}{C-100}\right)\right] && \text{for } 100\text{Å} < x < C \\ &= 0 && \text{for } x > C \end{aligned} \tag{13}$$

In Eq. 13, U^{Hyd} is expressed in mJ m^{-2}, B (expressed in units of mJ/m^2)=158, k (expressed in units of 1/Å)=10^{-4}, A (expressed in units of mJ/m^2)=40, C=15217.4 Å, and x is the separation distance in units of Å. It is important to reiterate here that Eq. 13 is merely a mathematical fit to the numerical results obtained from the model simulation, and is solely used to evaluate the integrals needed to obtain the bead–bead interaction forces and the consequent scaling relationships in explicit mathematical forms.

Results and discussion

Development of the scaling law

The dominantly exponential nature of $U^{Hyd,Sphere}$ essentially suggests that this somewhat resembles the form given by Eq. 1. In this regard, it is interesting to observe that the parameter R_{attr} in Eq. 1 appears to be a free parameter. However, we show here that this apparently free parameter solely dictates the interaction forces that drive the polymer condensation. To this end, we will exemplify the particular role of hydrophobic interactions, for which there appears to be a universal scaling relationship between the parameters R_{attr}/σ, $d_S^* = (r - 2a_{rad})/\sigma$, and a_{rad}/σ, which may be obtained by equating the form given by Eq. 1 with the results of Eqs. 11–13. A visual representation of the corresponding interrelationship is depicted in Fig. 2. It

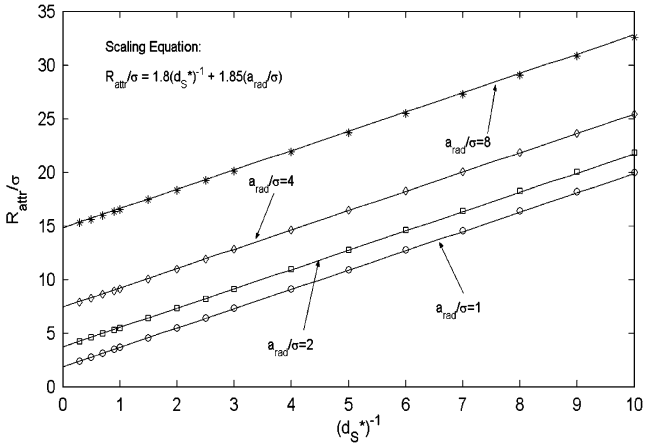

Fig. 2 Scaling variation of R_{attr}/σ with the inverse of dimensionless separation distance d_S^* and dimensionless radius a_{rad}/σ. The *continuous lines* represent variations given by Eq. 14, whereas the markers (*circles* for a_{rad}/σ=1, *squares* for a_{rad}/σ=2, *diamonds* for a_{rad}/σ=4, and *stars* for a_{rad}/σ=8) give the results obtained from the present simulation

may be inferred from Fig. 2 that the parameter R_{attr} need not necessarily be a constant, but may be sensitively dependent on the variations in d_S^* and a_{rad}/σ. R_{attr} is found to increase linearly with d_S^{*-1}. Such a phenomenon suggests that at smaller separation distances, the effects of disturbances to the distribution of the water molecules (the main source of solvophobic interactions)—as caused by the presence of a given solute in its neighborhood—are more likely to propagate in the vicinity of the other solute, thereby affecting the length scale of their overall attractive influences. On the other hand, R_{attr} increases with a_{rad}/σ for a given d_S^*, indicating that larger bead radii essentially amplify the effective domain of influence of hydrophobic interactions. Remarkably, the variations in R_{attr} are seen to obey the following universal characteristics:

$$\frac{R_{attr}}{\sigma} = 1.8\left(d_S^*\right)^{-1} + 1.85\left(\frac{a_{rad}}{\sigma}\right) \tag{14}$$

Equation 14 essentially suggests that hydrophobic interactions between spherical units can be captured by a potential of the form depicted by Eq. 1, with a modified solvation decay length, as given by Eq. 14. It is important to recognize that despite being apparently abstracted from the underlying complicated details in its functional form, Eq. 14 essentially represents the complex physics of bead–bead hydrophobic interactions. This is ensured by effective upscaling in which the background thermodynamic calculations merely play the role of a synthetic microscope for visualizing interactions between the fine-grain features and coarse-grain features of the pertinent interaction mechanisms.

Comparison with MDS results: validation of the proposed scaling law

To illustrate the effectiveness and validity of the proposed scaling of the solvation decay length, we compare the result of the present calculation with results from several MDS studies. Comparisons are made in a manner that highlights various important aspects of the proposed universal scaling law. The first and foremost statement of the scaling law is that it can reproduce the size dependence of the PMF (potential of mean force). To do this, we compare the PMF values (in vacuum) obtained using the present derivation with those obtained from MDS results [49, 50] corresponding to hydrophobic interactions of nonpolar dimers of four different organic molecules (namely isobutane, neopentane, bicyclooctane, and adamantane) at separation distances that make the repulsive contribution negligible. For these comparisons, we use $\widetilde{u}_0$ as the fitting parameter, which is estimated by comparing the results of the scaling calculation with the MDS result for a particular value of separation distance (see the caption of Fig. 3 for more details). The excellent agreement (see Fig. 3) of the PMF profiles for dimers of different sizes (for each of the four organic molecules, the molecular diameter is estimated as $\sigma_0 = r_c/2^{1/6}$, where the values of r_c are 0.52 nm, 0.58 nm, 0.62 nm and 0.68 nm for isobutane, neopentane, bicyclooctane and adamantane, respectively [49, 50]) between the results from the present calculation and the MDS results [49, 50] clearly establishes the usefulness of the present formalism for correctly predicting the size dependence of the PMF.

Having conclusively established the usefulness of the proposed scaling law for delineating the size dependence of the PMF, we now aim to show how this scaling law can successfully incorporate the solvent-interaction effect in the representation of the interspecies hydrophobic interactions without requiring the explicit calculation of the solvent dynamics. As we are only interested in the representation of correct attractive effects, we look to provide comparisons (with MDS results) for cases where repulsive interactions are negligible. Hence, we compare our simulation results with the results of the MDS study of Southall and Dill [51] (see Fig. 4). This comparison, in addition to again showing the capacity of the proposed scaling law to capture the size-dependent behavior of PMF, clearly demonstrates that it is possible to represent the solvent-interaction dependence of hydrophobic forces with the present formalism without the need to explicitly resolve the solvent–solvent interaction. It should be noted here that the potential (with the scaled solvation decay length) described in the present work is intended to capture the interactions of hydrophobic solutes at the mesoscopic scale. Standard mesoscopic simulations, which use a constant solvation decay length, cannot capture the reported solute-size dependence [49, 50] or the solvent-

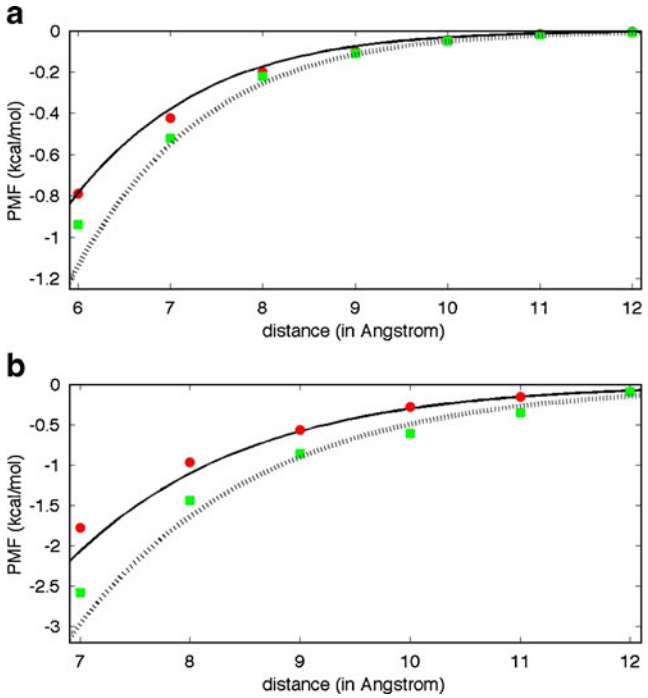

Fig. 3 **a** Comparison of the result from the present calculation of the size dependence of the PMF with the equivalent MDS result [49] (with the interactions considered to occur in vacuum). The *bold line* and the *dotted lines* are the results from the present calculation corresponding to hydrophobic interactions of nonpolar dimers of isobutane and neopentane, respectively. The markers (*red circles* for isobutane and *green squares* for neopentane) represent the corresponding results from MDS [49]. For the present simulation, the values of $\widetilde{u}_0$ are calculated as 0.020 J/m^2 and 0.017 J/m^2 for isobutane and neopentane, respectively (by matching with the MDS result corresponding to a distance of 9 Å [49]). **b** Comparison of the result from the present calculation of the size dependence of the PMF with the equivalent MDS result [50] (with the interactions considered to occur in vacuum). The *bold line* and the *dotted lines* are the results from the present calculation corresponding to hydrophobic interactions of nonpolar dimers of bicyclooctane and adamantane, respectively. The markers (*red circles* for bicyclooctane and *green squares* for adamantane) represent the corresponding results from MDS [50]. For the present simulation, the values of $\widetilde{u}_0$ are calculated as 0.036 J/m^2 and 0.031 J/m^2 for bicyclooctane and adamante, respectively (by matching with the MDS result corresponding to distance of 9 Å [50])

interaction dependence of the PMF [51]. In contrast, the proposed approach accounts for the PMF in a physically correct way, even in a mesoscopic model that does not provide explicit information on the individual moieties and may not explicitly characterize the behavior of the solvent. This, we believe, clearly demonstrates the importance and validity of the proposed scaling argument.

Usefulness of the proposed scaling law in molecular modeling

The need for molecular modeling stems from the inability of continuum modeling approaches to correctly represent certain phenomena when it is necessary to study the dynamics of all of the molecules involved. However, the excessive computational cost of molecular modeling often means that it is necessary to use mixed computational approaches (e.g., mesoscopic approaches like BDS, where the dynamics of solutes/particles are treated using the molecular approach but the details of the background solvent are coarse-grained) or a very small computational volume (e.g., to perform molecular modeling of an entire system that is very small and contains only a very limited number of solvent molecules). Thus, there have only rarely been studies where the solvent effects are explicitly accounted for in large systems. In this regard, our proposed scaling approach, by successfully addressing the solute-size dependence and solvent-interaction dependence of hydrophobic effects in a mesoscopic framework, could prove to be immensely important when developing numerical codes or potential software that are intended to handle large computational volumes but also to include solvent effects or solute-size effects in the overall calculations. Hence, in effect, our formalism is a step towards the development of a modified mesoscopic framework that performs calculations in a coarse-grained domain, but still considers the essential quantitative implications of solvent or solute sizes in the computational procedure.

It should be noted here that there have been several previous attempts to represent hydrophobic effects through such implicit solvent modeling [52–55]. The present

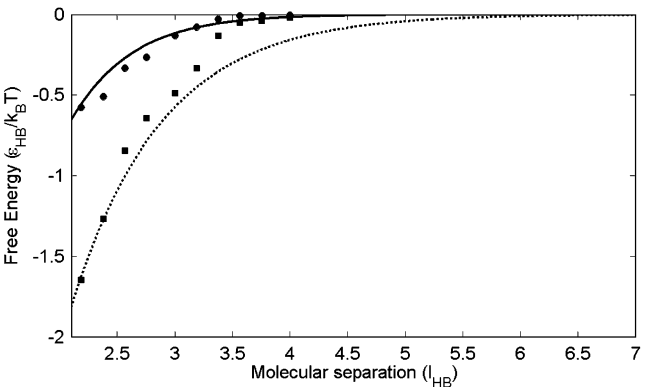

Fig. 4 Variation of the potential of mean force (PMF) (or free energy) with the distance between two spherical apolar solvophobic species. The energy is expressed in units of the hydrogen-bond interaction energy (ε_{HB}) of a water molecule (as described in [51]) and the distance in terms of the hydrogen-bond interaction length (l_{HB}). The results for the MDS simulation (obtained from [51]) are shown by markers (*circles* for solutes of diameter $1.5l_{HB}$ and *squares* for solutes of diameter $2l_{HB}$), whereas the results from the present simulation are depicted by lines (*continuous bold lines* for solutes of diameter $1.5l_{HB}$ and *dotted lines* for solutes of diameter 2 l_{HB}). The results were obtained with $\widetilde{u}_0\sigma^2$ equal to 0.05 (in units of ε_{HB}); this value of $\widetilde{u}_0\sigma^2$ is obtained by comparing with the MDS result [51] corresponding to a separation distance of 3.5 (in units of l_{HB})

approach is distinctive and more effective than those approaches in the sense that it condenses all of the implicit effects into a single universal mathematical representation of the hydrophobic decay length. Thus, for any system where hydrophobic effects dominate, Eqs. 1 and 14 and the correct value of $\widetilde{u}_0$ can be used to mimic the exact behavior of a hydrophobic solute in terms of the appropriate size dependence and solvent-interaction dependence. Hence, we provide a methodological basis for capturing hydrophobic effects at extremely small length scales (length scales where, otherwise, one invariably needs to explicitly represent solvent molecules) via mesoscopic approaches such as BDS. Also, our formalism can be viewed as the first step toward the development of efficient mathematical relationships for various other physical forces (incorporating the appropriate dependencies of system parameters), which will eventually lead to greater computational convenience in current molecular modeling strategies.

Conclusions

In this paper, we have provided a theoretical derivation that leads to a universal scaling relationship for the decay length that governs hydrophobic interactions, which are responsible for the strong attractive forces between structural units in poor solvents. Our calculation demonstrated that the hydrophobic decay length can act as an important guide when quantifying the underlying interactions, which is achieved by upscaling the pertinent thermophysical events that occur over reduced length scales. In particular, changing the distances between the individual hydrophobic units as well as the sizes of the interacting beads may strongly influence the strength of the consequent interaction forces, as shown by our proposed scaling law. By validating the proposed scaling law through comparison with MDS results, we demonstrated that the present formalism can successfully implement the size dependence and the solvent-interaction dependence of the hydrophobic attraction in an extremely effective computational framework that treats the solvent interactions in a coarse-grained manner. This should eventually pave the way for the development of improved mesoscopic simulation strategies that can be applied to hydrophobic interaction problems at extremely short system length scales, which would otherwise require that the solvent–solvent and solvent–solute interactions are captured explicitly.

References

1. Choudhury N, Pettitt BM (2005) J Am Chem Soc 127:3556–3567
2. Ametov I, Prestidge CA (2004) J Phys Chem B 108:12116–12122
3. Ananikian N, Ananakyan L, Artusoa R (2007) Phys Lett A 360:615–618
4. Huang X, Zhou R, Berne BJ (2005) J Phys Chem B 109:3546–3552
5. Goel G, Athawale MV, Garde S, Truskett TM (2008) J Phys Chem B 112:13193–13196
6. Huang X, Margulis CJ, Berne BJ (2003) Proc Nat Acad Sci USA 100:11953–11958
7. Zangi R, Hagen M, Berne BJ (2007) J Am Chem Soc 129:4678–4686
8. Vaitheeswaran S, Thirumalai D (2006) J Am Chem Soc 128:13490–13496
9. Dzubiella J, Hansen JP (2004) J Chem Phys 121:5514–5530
10. Bulone D, Martorana V, San Biagio PL, Palma-Vittorelli MB (1997) Phys Rev E 56:R4939–R4942
11. Bulone D, Martorana V, San Biagio PL, Palma-Vittorelli MB (1997) Phys Rev E 62:6799–6809
12. Fernández A (2002) Phys Lett A 299:217–220
13. Zbilut JP, Scheibel T, Huemmerich D, Webber CL Jr, Colafranceschi M, Giuliani A (2005) Phys Lett A 346:33–41
14. Galashev AY, Rakhmanova OR (2008) Phys Lett A 372:3694–3698
15. Silverstein KAT, Haymet ADJ, Dill KA (1998) J Am Chem Soc 120:3166–3175
16. Rajamani S, Truskett TM, Garde S (2005) Proc Nat Acad Sci USA 102:9475–9480
17. Qin Y, Fichthorn KA (2006) Phys Rev E 74:020401(R)(1–4)
18. Ashbaugh HS, Paulaitis ME (2001) J Am Chem Soc 123:10721–10728
19. Das T, Das S, Chakraborty S (2009) J Chem Phys 130:244904 (1–12)
20. Das S, Chakraborty S (2010) J Chem Phys 133:174904(1–15)
21. Montesi A, Pasquali M, Mackintosh FC (2004) Phys Rev E 69:021916(1–10)
22. Schnurr B, Mackintosh FC, Williams DRM (2000) Europhys Lett 51:279–285
23. Aranson IS, Tsimring LS (2003) Europhys Lett 62:848–854
24. Schnurr B, Gittes F, Mackintosh FC (2002) Phys Rev E 65:061904(1–13)
25. Lee SH, Kapral R (2006) J Chem Phys 124:214901(1–8)
26. Cooke IR, Williams DRM (2004) Macromolecules 37:5778–5783
27. Sabeur SA, Hamdache F, Schmid F (2008) Phys Rev E 77:020802 (R)(1–4)
28. Rapaport DC (2003) Phys Rev E 68:041801(1–11)
29. Polson JE, Moore NE (2005) J Chem Phys 122:024905(1–11)
30. Lee N, Thirumalai D (2001) Macromolecules 34:3446–3457
31. Kikuchi N, Gent A, Yeomans JM (2002) Eur Phys J E 9:63–66
32. Kikuchi N, Ryder JF, Pooley CM, Yeomans JM (2005) Phys Rev E 71:061804(1-8)
33. Pham TT, Bajaj M, Prakash JR (2008) Soft Matter 4:1196–1207
34. Polson JM, Zuckermann MJ (2000) J Chem Phys 113:1283–1293
35. Polson JM, Zuckermann MJ (2002) J Chem Phys 116:7244–7254
36. Frisch T, Verga A (2002) Phys Rev E 66:041807(1–11)
37. Chang RW, Yethiraj A (2001) J Chem Phys 114:7688–7699
38. Lum K, Chandler D, Weeks JD (1999) J Phys Chem B 103:4570–4577
39. Rowlinson JS, Widom B (1982) Molecular theory of capillarity. Clarendon, Oxford
40. Narten AH, Levy D (1971) J Chem Phys 55:2263–2269
41. Stillinger FH (1973) J Solution Chem 2:141–150
42. Pratt LR, Chandler D (1977) J Chem Phys 67:3683–3704
43. Hummer G, Garde S, García AE, Pohorille A, Pratt LR (1996) Proc Nat Acad Sci USA 93:8951–8955
44. Pratt LR, Pohorille A (1992) Proc Nat Acad Sci USA 89:2995–2999

45. Bhattacharjee S, Elimelech M, Borkovec M (1998) Croat Chem Acta 71:883–903
46. Eisenberg D, McLachan AD (1986) Nature 319:199–203
47. Juffer AH, Eisenhaber F, Hubbard SJ, Walther D, Argos P (1995) Protein Sci 4:2499–2509
48. Vallone B, Miele AE, Vecchini P, Chiancone E, Brunori M (1998) Proc Nat Acad Sci USA 95:6103–6107
49. Sobolewski E, Makowski M, Czaplewski C, Liwo A, Oldziej S, Scheraga HA (2007) J Phys Chem B 111:10765–10774
50. Makowski M, Czaplewski C, Liwo A, Scheraga HA (2010) J Phys Chem B 114:993–1003
51. Southall NT, Dill KA (2002) Biophys Chem 101–102:295–307
52. Chen J, Brooks CL III (2007) J Am Chem Soc 129:2444–2445
53. Cheng LT, Dzubiella J, McCammon JA, Li B (2007) J Chem Phys 127:084503
54. Chen J, Brooks CL III, Khandogin J (2008) Curr Opin Struct Biol 18:140–148
55. Chen J, Brooks CL III (2008) Phys Chem Chem Phys 10:471–481